Characteristics and Controlling Factors of Shale Oil Reservoir Spaces in the Bohai Bay Basin

DENG Yuan[1], CHEN Shiyue[1, *], PU Xiugang[2] and YAN Jihua[1]

[1] *School of Geosciences, China University of Petroleum(East China), Qingdao 266580, Shandong, China*
[2] *Research Institute of Exploration and Development, PetroChina Dagang Oilfield Company, Tianjin 300280, China*

Abstract: The Cenozoic continental strata of the Bohai Bay Basin are rich in shale oil resources, and they contain various types of reservoir spaces that are controlled by complex factors. Using field emission scanning electron microscopy (FE-SEM), automatic mineral identification and characterization system (AMICS), CO_2 and N_2 gas adsorption, and focused ion beam scanning electron microscopy (FIB-SEM), the types of shale reservoir spaces in the Bohai Bay Basin are summarized, the spatial distribution and connectivity of the various types of pores are described in detail, the microscopic pore structures are characterized, and the key geological mechanisms affecting the formation and evolution of the reservoir spaces are determined. Three conclusions can be drawn from the present study. First, the shale reservoir spaces in the Bohai Bay Basin can be divided into three broad categories, including mineral matrix pores, organic matter pores, and micro fractures. Those spaces can be subdivided into seven categories and fourteen sub-categories based on the distribution and formation mechanisms of the pores. Second, the complex pore-throat structures of the shale reservoir can be divided into two types based on the shape of the adsorption hysteresis loop. The pore structures mainly include wedge-shaped, flat slit-shaped, and ink bottle-shaped pores. The mesopores and micropores are the main contributors to pore volume and specific surface area, respectively. The macropores provide a portion of the pore volume, but they do not significantly contribute to the specific surface area. Third, the factors controlling the development of microscopic pores in the shale are complex. The sedimentary environment determines the composition and structure of the shale and provides the material basis for pore development. Diagenesis controls the types and characteristics of the pores. In addition, the thermal evolution of the organic matter is closely related to inorganic diagenesis and drives the formation and evolution of the pores.

Key words: reservoir characteristic, pore structure, controlling factor, shale oil, Bohai Bay Basin

E-mail: dengyuan_upc@163.com

1 Introduction

Since the successful commercial development of shale gas in North America, there has been an upsurge in the exploration and development of unconventional hydrocarbon resources worldwide, which has promoted the development of unconventional hydrocarbon geology (Macquaker and Adams, 2003; Nelson, 2009; Aplin and Macquaker, 2011; Li et al., 2016; Chen F.W., et al., 2018; Chen X.H., et al., 2018a, 2018b; Bao et al., 2018; Zhai et al., 2018a). Shale oil is an unconventional energy source, but it is not as common as shale gas in commercial exploitation. The US Energy Information Administration (EIA) estimates that the shale oil resources recoverable with technology can reach 44.8×10^8 t in China, which is second only to the United States and Russia. By the end of 2016, a production capacity of 155.3×10^4 t was achieved (Zou et al., 2015; Jia, 2017; Hu et al., 2018), demonstrating significant exploration potential. China's shale oil resources are mainly located in the Bohai Bay Basin, Songliao Basin, Junggar Basin, Santanghu Basin, and Ordos Basin (Liu et al., 2015, 2018; Zhang et al., 2016a; Yang et al., 2017; Song et al., 2017; Zhao et al., 2018). Among them, the Cenozoic continental strata of the Bohai Bay Basin contain an enormous amount of shale oil resources. Thus far, breakthroughs have occurred in the Kongdian Formation in the Cangdong Depression and in the Shahejie Formation in the Jiyang Depression. For example, after fracturing, well GD6x1 in the Cangdong Depression, reached a daily oil production of 28 t, and well G1608 reached a daily oil production of 7 t. By the end of 2016, hydrocarbons were found in the shale sections of more than 800 exploration wells and industrial hydrocarbon flows were obtained in 37 exploration wells in the Jiyang Depression, including well H54 in the Dongying Depression, which had a cumulative production of 28×10^3 t. Similarly, wells L42 and XYS9 in the Zhanhua Depression had a cumulative production of more than 10×10^3 t (Sun et al., 2017; Zhou et al., 2018).

Unlike the goal of conventional hydrocarbon exploration, which is primarily to locate traps, the goal of shale oil exploration is to identify favorable reservoirs due to the “source-reservoir integration” characteristics. Shale is mainly composed of minerals with particle sizes of less than 62.5 μm. Compared with conventional sandstone reservoirs, shale reservoirs have low porosity and low permeability, small pore-throat size, complex pore structure, and strong heterogeneity. Therefore, conventional reservoir testing techniques cannot be effectively applied to shale oil reservoirs (Lin, 2016). To accurately characterize the shale reservoir space, which is

This article has been accepted for publication and undergone full peer review but has not been through the copyediting, typesetting, pagination and proofreading process, which may lead to differences between this version and the Version of Record. Please cite this article as doi: 10.1111/1755-6724.14286.

dominated by micrometer-nanometer-sized pore-throats, more accurate testing methods with higher resolutions are needed (Milner et al., 2010; Chalmers and Bustin, 2012). Current research methods for shale reservoir analysis can be divided into qualitative and quantitative methods. The qualitative characterization method, which mainly uses field emission scanning electron microscopy (FE-SEM), atomic force microscopy (AFM), computed tomography (CT) scanning, and focused ion beam scanning electron microscopy (FIB-SEM) to directly observe the shale pores and to obtain information on the pore type, size, and distribution (Desbois et al., 2009; Loucks et al., 2009, 2012; Zou et al., 2011; Curtis et al., 2012a; Javadpour et al., 2012; Chalmers et al., 2012; Bai et al., 2013). The quantitative characterization method, which mainly uses gas adsorption, high-pressure mercury injection capillary pressure (MICP), and nuclear magnetic resonance (NMR) to indirectly calculate the pore size distribution, pore morphology, and pore connectivity of shale (Slatt and O'Brien, 2011; Curtis et al., 2012b; Schmitt et al., 2013; Mastalerz et al., 2013; Rexer et al., 2014). When multiple methods are used in testing, the resolution and representativeness of the samples need to be taken into account, and to rationally integrate the data obtained from the different methods (Zhu et al., 2016; Wu et al., 2018).

However, there is still a large gap between the capability of shale oil exploration in the Bohai Bay Basin to that in North America. The main reason for this gap is the lack of adequate research on the shale reservoir in the Bohai Bay Basin. Moreover, the lack of systematic information on key topics such as the types of shale reservoir space, the main factors controlling reservoir development, and diagenetic evolution, contribute to this gap. This study summarizes the types of microscopic pores in the shale reservoirs in the Bohai Bay Basin, clarifies the spatial distribution and connectivity of the various types of pores, and analyzes the key geologic mechanisms affecting the formation and evolution of reservoir space. The objective of this paper is to provide theoretical support for the next steps in shale oil exploration in the Bohai Bay Basin.

2 Samples and Methods

2.1 Geologic setting and samples

The Bohai Bay Basin is one of the most important petroliferous basins in eastern China (Fig. 2). The basin contains seven depressions, which are the Liaohe, Jizhong, Huanghua, Jiyang, Linqing, Bozhong, and Liaodong Bay depressions (Teng et al., 2014; Zhao et al., 2015). The Paleogene Bohai Bay Basin was formed in a fault depression period when lacustrine sediments were frequently deposited in low-lying areas throughout the Basin. Among these basins, the shale with oil exploration potential is mainly concentrated in the Jiyang Depression, the Liaohe Depression, the Shahejie Formation within the Dongpu Depression, and the Kongdian Formation within the Cangdong Depression in the Huanghua Depression. These shales are generally rich in organic matter, which is widely distributed very thick and has stable preservation. In this study, samples collected from the lacustrine facies shale are from two sources. These sources include the second member of the Kongdian Formation within the Cangdong Depression in the Huanghua Depression (Wells GX, GDA, and GDB) and the third and fourth member of the Shahejie Formation within the Dongying Depression in the Jiyang Depression (Wells FY1, LY1). The locations of the samples collected in this study are shown in Figure 1.

2.2 Geochemical and mineral analyses

Total organic carbon (TOC) content analyses of the shale samples were conducted using a Leco CS-230 at the Zhongyuan Oilfield Exploration and Development Research Institute. Prior to testing, samples >10 g were ground to <0.2 mm, placed in a dilute hydrochloric acid solution at 60–80°C for more than 2 h, and then dried to remove the carbonate components of the sample. X-ray diffraction (XRD) analyses were carried out using a Rigaku D/max-2500 X-ray diffractometer at the China University of Petroleum (East China). First, the samples were ground to < 80 μm, and then they were analyzed using the method of Hillier (2002).

2.3 FE-SEM, AMICS, and FIB-SEM

The microscopic pores of the shale were observed using a Zeiss Merlin Gemini2 FE-SEM. In order to obtain nanometer flatness of the sample surface, Ar-ion milling was performed using a Leica EM RES 102 for more than 5 h prior to analysis. Next, the sample was placed in the FE-SEM for observation and imaging at a 1.5 kV accelerating voltage. The FE-SEM was equipped with a secondary electron detector, a backscatter electron detector, and an energy dispersive spectrometer (EDS) to obtain the surface morphology and mineral composition of the sample. The automatic mineral identification and characterization system (AMICS) used an EDS equipped with an FE-SEM to surface-scan specific areas of the sample. AMICS software was then used to automatically identify and quantify the minerals present in each sample. Prior to the experiment, the surface of the sample was coated with carbon using a Leica EM ACE 200. The three-dimensional (3D) spatial distribution of the microscopic pores of the shale was determined using a Zeiss Crossbeam 540 FIB-SEM. First, the back scattered electron (BSE) mode was used to observe and select the target area, and then, the sample stage was rotated 52° to orient the ion beam perpendicular to the sample's surface. The surface of the target area was sprayed with Pt to reduce the damage caused by the ion beam. Next, the sample was continuously cut at a spacing of 5–10 nm using a 30 kV gallium ion beam. The sample was imaged by the ion beam after each cut. Finally, the obtained slice images were subjected to 3D reconstruction. The above FE-SEM, AMICS, and FIB-SEM analyses were all conducted in the Micro-Nanostructure Imaging Laboratory at the Institute of

Geology and Geophysics, Chinese Academy of Sciences.

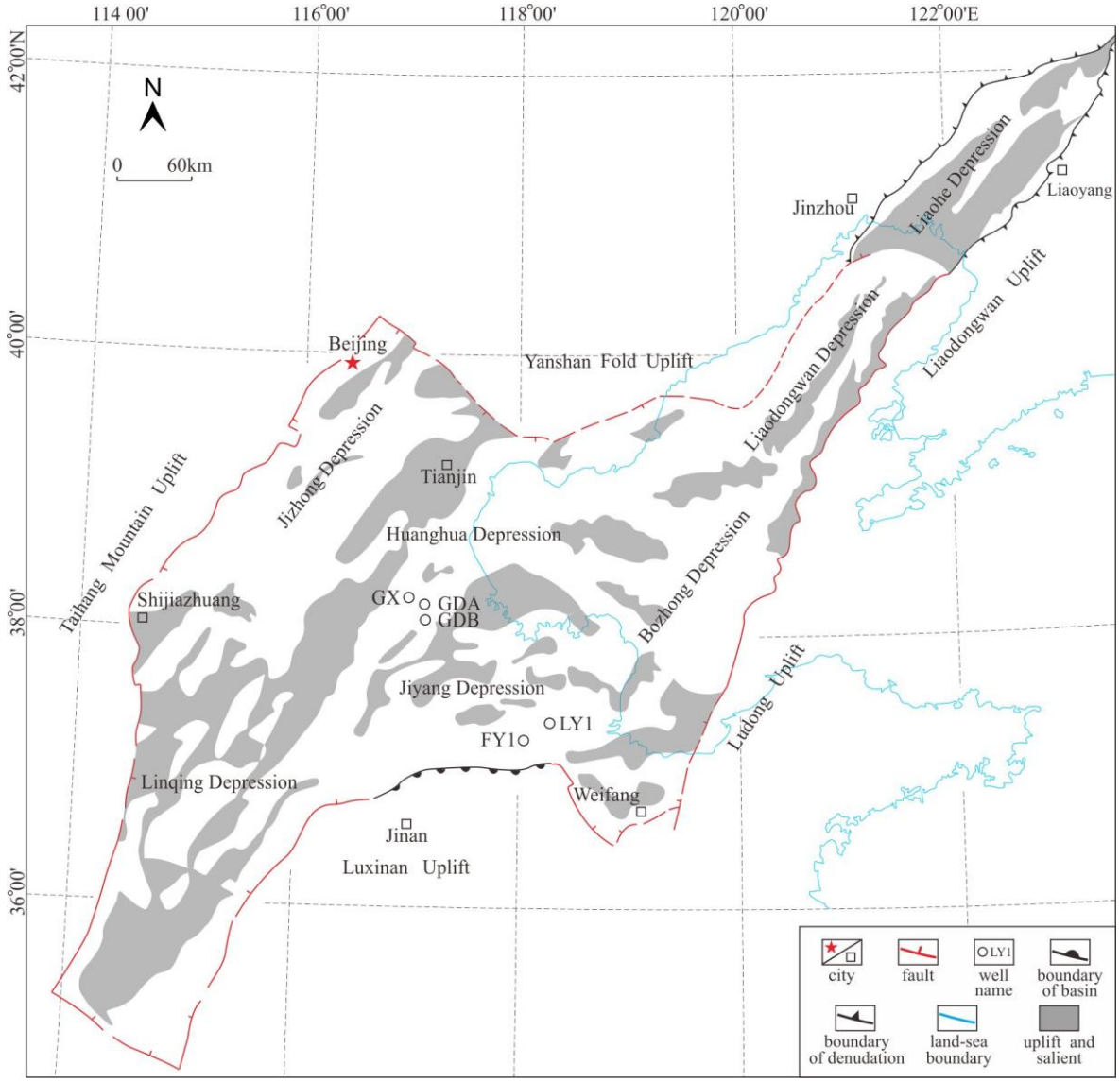

Fig. 1. Location of sampling wells and regional tectonic profile of the Bohai Bay Basin.

2.4 Low-temperature CO_2 and N_2 adsorption

The shale cryogenic gas adsorption was conducted at the Beijing Center for Physical and Chemical Analysis. The low-temperature CO_2 and N_2 adsorption experiments were carried out using a Nova 4200e Surface Area Analyzer and Pore Size Analyzer (Quantachrome, USA). The sample was pulverized to 150–250 μm and thoroughly dried. The sample was maintained at the temperature of liquid nitrogen (77.35 K at 101.3 kPa) to measure the N_2 adsorption. The temperature was maintained at 273.15 K for the CO_2 adsorption measurements. The pore volume, specific surface area, and pore size distribution of the micropores (< 2 nm) were obtained from the low-temperature CO_2 adsorption experiment. The pore volume, specific surface area, and pore size distribution of the mesopores and macropores (> 2 nm) were obtained from the low-temperature N_2 adsorption experiments (Gregg and Sing, 1982; Mastalerz et al., 2012, 2013). Following these experiments, the pore structure characteristics of the shale samples with different pore sizes were characterized.

3 Results

3.1 Basic shale characteristics

In the United States, shale oil is produced from marine shale formations, which are widely distributed. These formations are relatively thin bedded and weakly affected by terrestrial sources, have high organic matter content, decent types of organic matter, moderate thermal maturity, and weak reservoir heterogeneity. In contrast, the shale oil in the Bohai Bay Basin is mainly developed in the continental shale strata. As a result, the Bohai Bay Basin shale oil has a limited distribution, but it is very thick. The sedimentation processes were strongly influenced by a terrestrial source, and therefore the organic matter contents and types are heterogeneous, the

thermal maturity is low, Ro is generally below 1.0, and the reservoir is overall extremely heterogeneous (Table 1) (Zhao et al., 2018). The petrographic investigation of 120 samples show that the shale in the Bohai Bay Basin is mainly composed of detrital minerals, carbonate minerals, and clay minerals. The average amount of detrital minerals, such as quartz and feldspar, is 33.3%, whereas the average amount of carbonate minerals (calcite and dolomite) is 35.8% and the average amount of clay minerals is 23.1%. The shale also contains a small amount of pyrite and analcite based on the rock classification scheme of Yan et al. (2015) (Fig. 2a). The microscopic, SEM and AMICS images show that the quartz is primarily derived from a provenance outside of the basin. Generally, the quartz is striped or laminated, and there is almost no authigenic quartz (Figs. 2b and 2c). The carbonate mineral content is high, generally, more than 30%. The carbonate minerals are primarily formed by biochemical activity and likely underwent various degrees of recrystallization after deposition (Figs. 2d and 2e). In addition, mixed deposition is very common. The terrigenous detrital minerals and the carbonate minerals are both compositionally and structurally mixed. As a result, a lamina that appears to be made of a single component is usually composed of two or more minerals (Figs. 2f, 2g and 2h).

Table 1 Geological characteristics of marine shale in the United States and lacustrine shale in the Bohai Bay Basin

Type	Basin/Depression	Layer	Thickness (m)	Source rock characteristics			Reservoir characteristics	
				TOC (%)	OM type	Ro (%)	Porosity (%)	Permeability(mD)
Marine shale	Fort Worth	Barnett	15–60	5–8	II	0.6–1.4	4–10	0.02–0.10
	Williston	Bakken	3–15	7.2–10.6	I, II	0.6–1.2	8–12	0.05–0.50
	Western Culf	Eagle Ford	20–60	2.0–9.2	II	0.7–1.3	2–12	<0.01
Bohai Bay Basin lacustrine shale	Jiyang Depression	Es_3^L	50–400	0.6–16.3	I, II_1	0.5–0.9	2–8	0.05–0.50
		Es_4^U	50–400	0.6–16.7	II_1	0.5–1.1	1.3–9.3	0.04–1.90
	Liaohe Depression	Es_3	50–500	1.0–17.1	II, III	0.5–1.3	11.4	0.01–0.27
	Dongpu Depression	Es_3^U	90–580	0.5–7.8	I, II_1	0.6–0.8	3.4–5.4	0.01–0.10
	Cangdong Depression	Ek_2	80–400	0.3–12.9	I, II_1	0.6–1.3	3.2–8.3	0.01–1.62

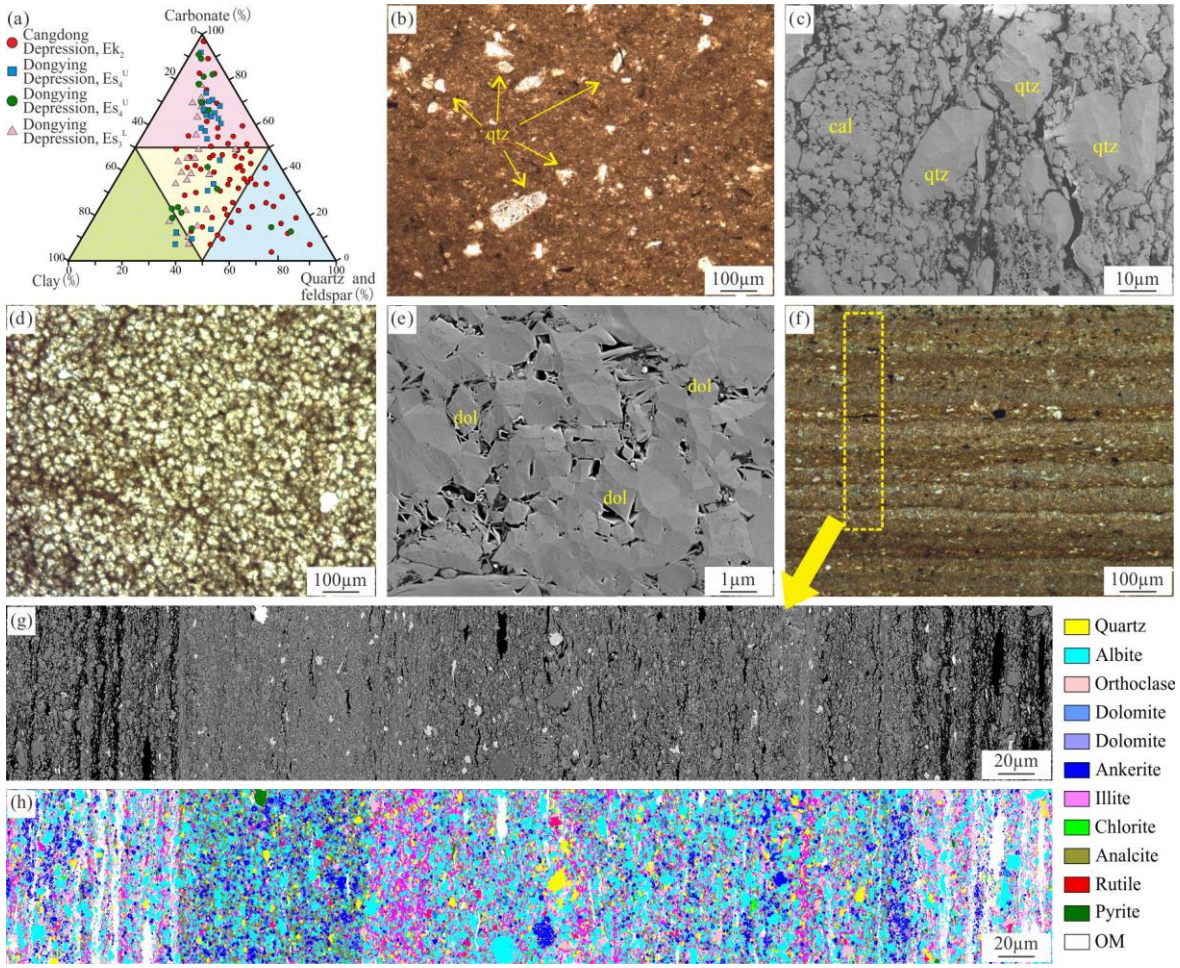

Fig. 2. Classification and mineral characteristics of the shale in the Bohai Bay Basin.
(a) Classification of the shale in the Bohai Bay Basin; (b) Detrital quartz combined with clay minerals in sample GX-7-7, 3054.55 m; (c) Quartz and calcite in sample GX-19, 3116.01 m; (d) Dolomite in sample GX-2-73, 2942.3 m; (e) Dolomite combined with analcite in sample GX-2-73, 2942.3 m; (f) Various lamina in sample GX-6, 2977.05 m; (g) BSE image of the selected area in sample GX-6, 2977.05 m; (h) AMICS micrograph showing the mineral distribution of sample GX-6, 2977.05 m. qtz, Quartz; cal, Calcite; dol, Dolomite; anl, Analcite.

3.2 Types of reservoir space

At present, classification schemes for shale reservoir space are based on pore size, pore occurrence-structure, and pore origin (Rouquerol et al., 1994; Loucks et al., 2012; Yu, 2013; Wei et al., 2018). Among them, one pore size classification is the scheme proposed by the International Union of Pure and Applied Chemistry (IUPAC). In this classification scheme, shale pores were divided into micropores (less than 2 nm), mesopores (2–50 nm) and macropores (greater than 50 nm). The classification based on pore occurrence-structure is currently the most widely used classification scheme. Based on the classification schemes for multiple regions, in order to accurately characterize the diversity of the microscopic pores of the s Bohai Bay Basin shale, the shale pores are divided into three large classes: mineral matrix pores, organic material (OM) pores, and micro fractures (Table 2). According to their locations, the mineral matrix pores are divided into intergranular (interP) pores, intragranular (intraP) pores, intercrystalline pores, and dissolution pores. The OM pores are mainly secondary pores generated during the thermal evolution of organic matter. The micro fractures can be subdivided into structural micro fractures and diagenetic contraction micro fractures. Further division into subclasses can be completed based on the genetic mechanism of the pores. For example, intercrystalline pores include intercrystalline pores within pyrite, intercrystalline pores within calcite, and intercrystalline pores within dolomite.

Table 2 Classification of the pores in the Bohai Bay Basin shale

Large class	Class	Subclass	Formation mechanism
Mineral matrix pores	InterP pores	InterP pores between rigid particles	Primary compaction and particle accumulation
		InterP pores between rigid particle and ductile particle	
	IntraP pores	Clay intraP pores	Clay transformation and dehydration
	Intercrystalline pores	Intercrystalline pores within pyrite	Cementation
		Intercrystalline pores within calcite	Recrystallization
		Intercrystalline pores within dolomite	Dolomitization
	Dissolution pores	Dissolution pores within feldspar	Kerogen pyrolytic hydrocarbon generation and expulsion and clay transformation
		Dissolution pores within calcite	
		Dissolution pores within dolomite	
OM pores	OM pores	Intra-OM pores	Kerogen pyrolytic hydrocarbon generation and expulsion
		Inter-OM pores	
Micro fractures	Structural micro fractures		Tectonic stress action
	Diagenetic contraction fractures	Clay contraction fractures	Clay transformation and dehydration
		OM marginal fractures	Kerogen pyrolytic hydrocarbon generation and expulsion

3.2.1 Mineral matrix pores

(1) InterP pores

InterP pores refer to the pore spaces between mineral particles. They are mainly residual primary pores that remain after compaction and cementation (Loucks et al., 2012). Some of the interP pores in the continental shale of the Bohai Bay Basin were developed between brittle minerals (e.g., felsic and carbonate minerals) with strong compaction resistance (Fig. 3a). They are primarily triangular, polygonal, or irregular in shape with average pore sizes of a few hundred nanometers to a few micrometers. The rest of the pores were developed between brittle minerals and clay minerals (Figs. 3b and 3c). They are primarily linear and slit type pores with a small average pore size, and they are mostly nanopores. The interP pores typically have good connectivity.

(2) IntraP pores

The study area primarily contains intraP pores in clay minerals, i.e., parallel plate-shaped, wedge-shaped, or irregular-shaped intraP pores in illite, illite/smectite mixed layer, and chlorite (Figs. 3c and 3d) (Xi et al., 2016). The formation of intraP pores is not only related to the flocculent or lamellar crystal morphology of the clay minerals, but it is also related to the diagenetic transformation of clay minerals. They mainly consist of the micropores generated during the transformation from montmorillonite to illite/smectite mixed layer to illite (Zhang et al., 2018a). Despite the strong plasticity of clay minerals, the "cardhouse structure" formed by the angular contacts between the ore slices formed from the intraP pores in the clay minerals are partially preserved after compaction. The intraP pores are usually small in size, have widths of several nanometers to several tens of nanometers, have lengths of a few micrometers, and are filled with organic matter or pyrite.

(3) Intercrystalline pores

Intercrystalline pores are formed by loose packing or lattice defects during crystal growth, and they can be divided into pyrite intercrystalline pores (Fig. 3e), calcite intercrystalline pores, and dolomite intercrystalline pores (Fig. 3f). Pyrite is very common in shale that was formed in anoxic environments. The pyrite in the study area is framboidal and spherulitic. The framboidal druse is conducive to the development and preservation of intercrystalline pores (Huang et al., 2015; Liang et al., 2016). The intercrystalline pores of the calcite and dolomite are related to recrystallization and dolomitization. The intercrystalline pores are generally small in size and are often a few tens of nanometers wide. These pores have strong compaction resistance and tend to be

well-preserved.

(4) Dissolution pores

Under the influence of the organic acids and inorganic acids released by the thermal evolution of the organic material in the pores, unstable minerals, such as feldspar, calcite, and dolomite, are prone to dissolution. This process ultimately forms dissolution pores. The dissolution pores develop inside and on the edges of the minerals. Inside the grain, punctate, polygonal, or elliptical dissolution pores with pore sizes ranging from a few nanometers to several tens of nanometers are primarily develop (Figs. 3g and 3i). On the edges of the grains, harbor-shaped or irregularly shaped large dissolution pores (mostly micron-sized) commonly developed (Figs. 3h and 3i). The development of dissolution pores is mainly affected by the dissolution strength and the unstable mineral content. When strong dissolution occurs, the dolomite and calcite may be completely dissolved to form mold pores. Unstable minerals, such as carbonate minerals, are the material basis for dissolution pores. Thus, the higher the unstable mineral content, the more developed the dissolution pores. Generally, the dissolution pores are isolated pores with poor connectivity; however, when strong dissolution occurs, they can become connected to interP pores and OM pores to form ink bottle-shaped pores.

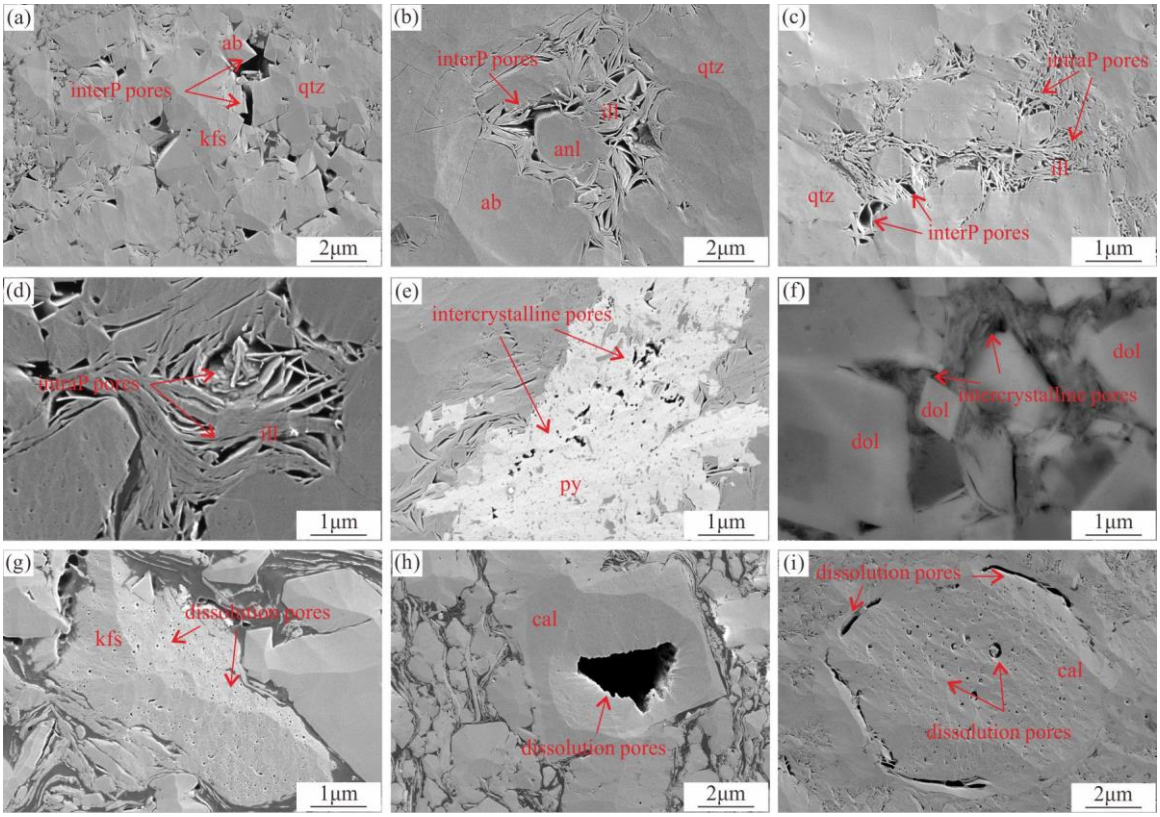

Fig. 3. Characteristics of the mineral matrix pores in the shale of the second member of the Kongdian Formation in the Cangdong Depression, Bohai Bay Basin.

(a) InterP pores between rigid particles in sample GX-7, 2977.18 m; (b) InterP pores between rigid particles and ductile particles in sample GX-19, 3124.61 m; (c) InterP pores between rigid particles and ductile particles, and intraP pores in clay in sample GX-8, 2977.3 m; (d) Clay intraP pores in sample GX-2, 2969.72 m; (e) Intercrystalline pores within the pyrite in sample GX-2, 2969.72 m; (f) Intercrystalline pores within the recrystallized dolomite in sample GX-8, 2977.3 m; (g) Dissolution pores within feldspar in sample GX-10, 2978.82 m; (h) Dissolution pores within the calcite in sample GX-3, 2971.1 m; (i) Dissolution pores within the calcite in sample GX-4, 2974.74 m. qtz, Quartz; ab, Albite; kfs, K feldspar; anl, Analcite; ill, Illite; py, Pyrite; dol, Dolomite; cal, Calcite.

3.2.2 OM pores

OM pores are secondary pores formed by the thermal evolution and hydrocarbon generation of the organic matter in the shale (Curtis et al., 2012a). These pores can be divided into internal pores and marginal pores based on their location (Figs. 4a and 4b), which is dependent on the difference in their pathways of thermal evolution during hydrocarbon generation of various types of kerogen. The shale in the study area is dominated by type I and type II kerogen. Type I kerogen generates hydrocarbon primarily through depolymerization, which forms the internal OM pores. In contrast, type II kerogen generates hydrocarbon through depolymerization and parallel defunctionalization, which produces the internal OM pores and edge pores (Ma et al., 2017). The internal OM pores are mostly round, elliptical, bubble-like, and irregular, while the organic matter edge pores are mainly slit-like or mesh-like. In addition, the number and morphology of the pores are also affected by adjacent minerals. For example, organic matter easily combines with clay minerals to form an organic-clay aggregate, and the clay mineral transformation process can catalyze the hydrocarbon generation of the organic matter, which further develops the OM pores in the aggregate (Fig. 4c) (Brooks, 1952; Johns, 1979).

Based on information gained from marine shale gas exploration, OM pores are the most important pore type in shale (Chen et al., 2018c). However, thermal evolution simulation experiments indicate that OM pores only form after a certain maturity (Ro > 0.6%), and their degree of development increases as the maturity of the organic matter increases (Fishman et al., 2012; Milliken et al., 2013). Compared with high-maturity marine shale, the Cenozoic shale in the Bohai Bay Basin has a relatively low thermal evolution, and it is generally within the oil-generation window (Ro = 0.7–1.2%). Moreover, it contains a small number of small diameter OM pores with poor connectivity (Zhai et al., 2017). The pores are unevenly distributed in isolation and are not dominant among the overall microscopic pores.

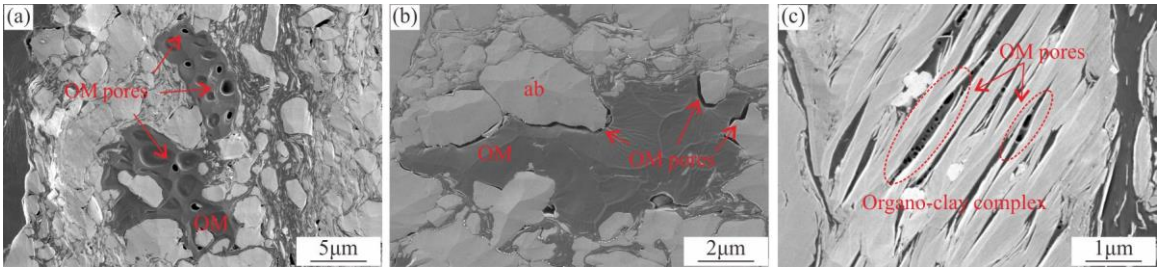

Fig. 4. Characteristics of the OM pores in the shale of the second member of the Kongdian Formation within the Cangdong Depression, Bohai Bay Basin.

(a) Internal OM pores in sample GX-14, 3109.86 m; (b) OM edge pores in sample GX-19, 3124.61 m; (c) OM pores within organo-clay complex (location indicated by red dots) in sample GX-6, 2977.05 m. ab, Albite; OM, organic matter.

3.2.3 Micro fractures

The micro fractures in the shale in the study area are very well developed and include structural micro fractures, clay contraction fractures, and organic matter marginal fractures. The structural micro fractures are mainly controlled by tectonic events and are irregularly distributed. The fracture surfaces form a jagged pattern and can usually extend for several micrometers to several tens of micrometers (Fig. 5a). The diagenetic contraction fractures are primarily associated with the clay minerals and were formed by a reduction in volume during the transformation of montmorillonite into illite (Fig. 5b). The organic matter marginal fractures are relatively small and are primarily located at the edge of the interface between the organic matter and the clay or brittle minerals. These fractures have a width of no more than 1μm (Fig. 5c). They are produced by a reduction in volume due to hydrocarbon expulsion and shrinkage during the thermal evolution of the organic matter. The micro fractures usually have good extensibility, and they can be used as a reservoir space for hydrocarbon as well as to connect pores of different scales and levels. They may act as channels for hydrocarbon migration from the microscopic pores to the macroscopic fractures, which jointly forms a complex stereoscopic pore network for the shale oil reservoir (Gale et al., 2007).

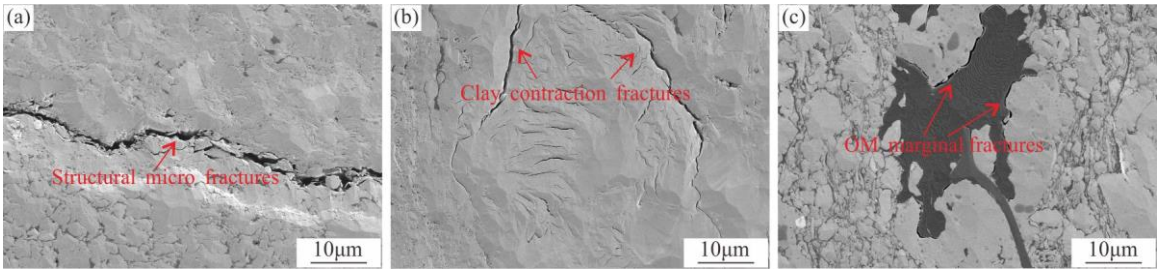

Fig. 5. Characteristics of micro fractures in the shale of the second member of the Kongdian Formation in the Cangdong Depression, Bohai Bay Basin.

(a) Structural micro fractures in sample GX-10, 2978.82 m; (b) Clay contraction fractures in sample GX-11, 2978.87 m; (c) OM marginal fractures in sample GX-3, 2971.1 m.

3.3 Distribution and connectivity of reservoir spaces

The various pores and micro fractures in the shale are not isolated. Instead, they are spatially combined and form a complex pore network within the continental shale. The connectivity between the pores is critical for the storage and migration of hydrocarbons (Zhang et al., 2018b). Two shale samples (GX-11 and GX-12) from the second member of the Kongdian Formation within the Cangdong Depression have large differences in mineral composition and organic matter content. Their 3D reservoir spaces were reconstructed using the FIB-SEM technique (Gu et al., 2015). In particular, sample GX-11 is massive and primarily composed of felsic and carbonate minerals, with a total mineral content of 87.3% and almost no organic matter. Sample GX-12 has a laminated structure, a felsic mineral content of 26.2%, a carbonate mineral content of 37.7%, a clay mineral content of 36.1%, and an organic matter content of 2.78%. To observe the distribution characteristics of the reservoir spaces, we conducted an advanced translucent rendering of the 3D model. The results before and after the rendering are compared in Figures 6e (rendering) and 6f (not rendered). The results of the FIB-SEM analyses indicate that the total porosity of sample GX-11 is 4.11%, of which micro fractures account for 0.27%.

The types of reservoir space mainly include interP pores and intraP pores, which are evenly distributed in space and are interconnected via long narrow micro fractures, resulting in good overall connectivity within the reservoir space (Fig. 6). The total porosity of sample GX-12 is 1.22%, of which micro fractures account for 0.26%. The reservoir space is dominated by intraP pores and OM pores. The pores are mostly isolated (Fig. 7) and their connectivity is inferior to that of sample GX-11.

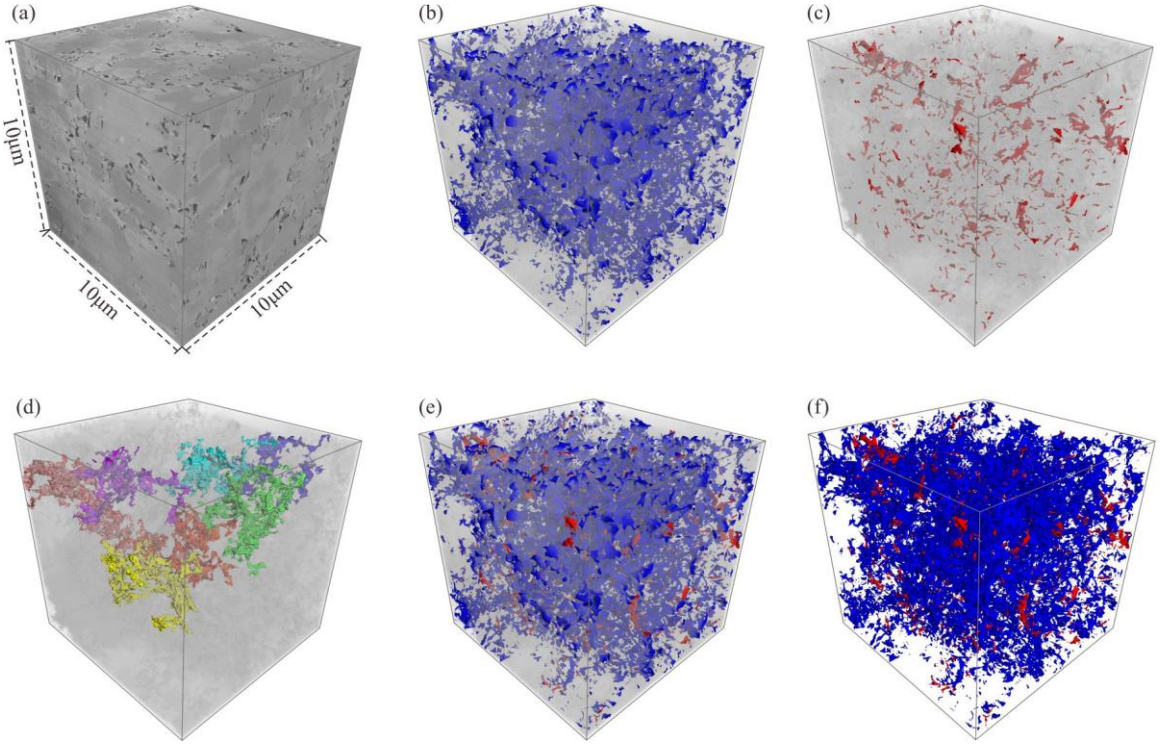

Fig. 6. FIB-SEM reconstructed images of sample GX-11 from the second member of the Kongdian Formation within the Cangdong Depression, Bohai Bay Basin.

(a)3D reconstructed image of sample GX-11, 2978.87 m; (b) Pores; (c) Micro fractures; (d) Connected pores. Each color represents a different connected pore network; (e) Total reservoir space (pores and micro fractures) after rendering; (f) Total reservoir space (pores and micro fractures) without rendering.

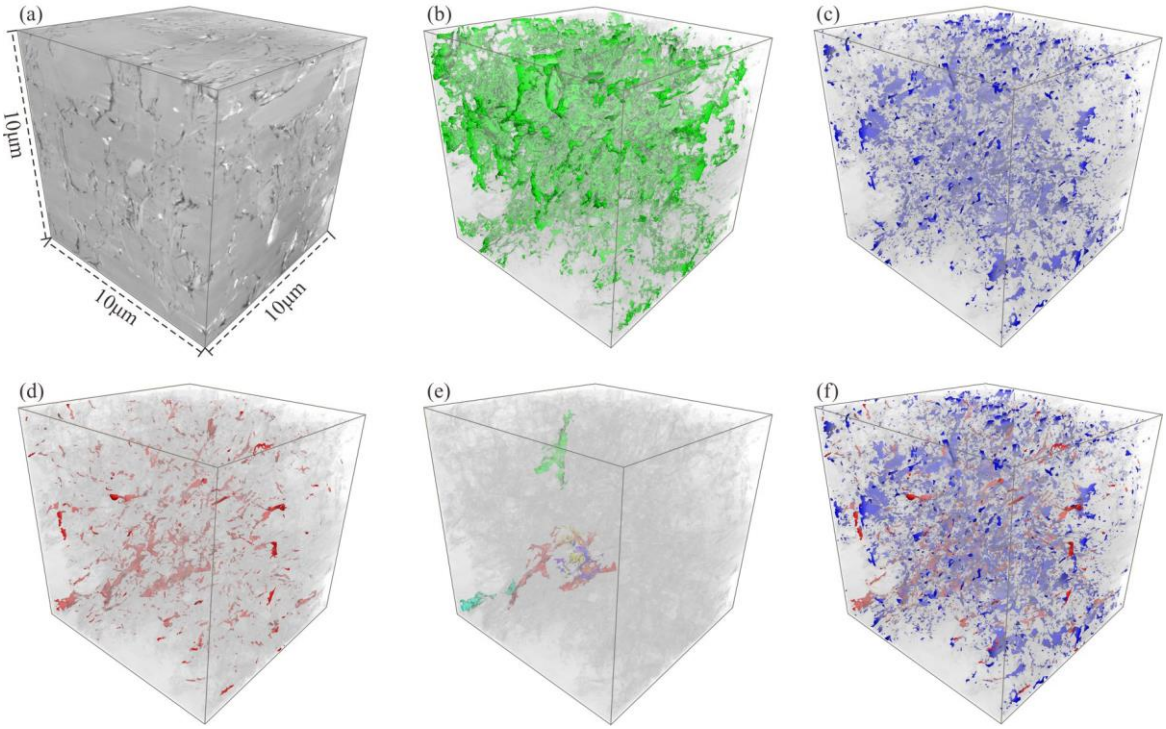

Fig. 7. FIB-SEM reconstructed image of sample GX-12 from the second member of the Kongdian Formation within the Cangdong Depression, Bohai Bay Basin.

(a) 3D reconstructed image of sample GX-12, 2979.21 m; (b) Organic matter; (c) Pores; (d) Micro fractures; (e) Connected pores. Each color represents a different connected pore network; (f) Total reservoir space (pores and micro fractures).

3.4 Characteristics of pore structure

3.4.1 CO_2 and N_2 absorption/desorption curves

Taking the shale samples from the second member of the Kongdian Formation within the Cangdong Depression and the Shahejie Formation in the Dongying Depression as an example, we found that the CO_2 adsorption curves were consistent with the type I adsorption isotherm defined by the International Association of Purification and Application (IUPAC) (Brunauer et al., 1938; Chen et al., 2017) (Fig. 8a). That is, as the relative pressure (P/P_0) increases, a monolayer of CO_2 molecules is absorbed and the amount of adsorption increases slowly until it reaches saturation. This phenomenon indicates that a certain number of micropores exist within a rock, which leads to micropore filling. The saturated adsorption is the micropore filling volume.

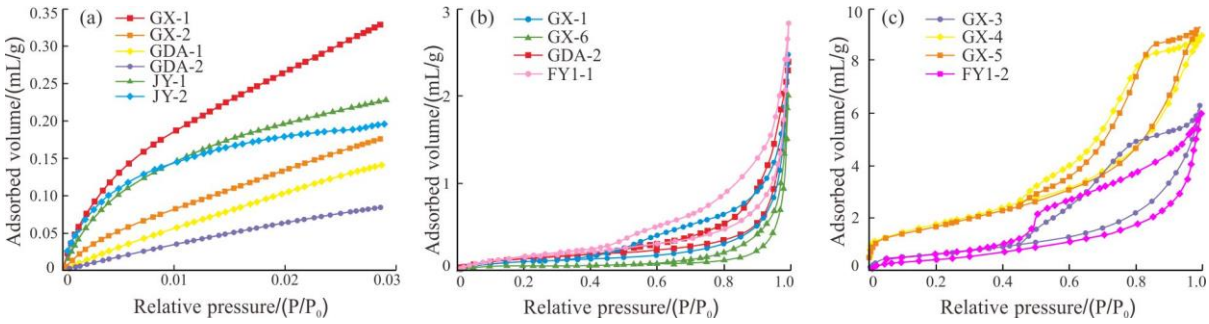

Fig. 8. CO_2 and N_2 absorption/desorption isotherms for the shale in the Bohai Bay Basin.
(a) CO_2 adsorption curve; (b) N_2 absorption/desorption curve of the first type of sample; (c) N_2 absorption/desorption curve of the second type of sample.

All of the N_2 adsorption isotherms exhibit a three-section inverse S shape, which matches the IUPAC-defined type II adsorption isotherm (Figs. 8b and 8c). The first section of the adsorption isotherm ($P/P_0<0.6$) slowly increases and is slightly convex upward, denoting the transition from monolayer adsorption to multi-molecular-layer adsorption. The middle section ($0.6<P/P_0<0.9$) is concave and increases rapidly, exhibiting the characteristics of multi-molecular-layer adsorption. The end section ($P/P_0>0.9$) increases abruptly, and no saturated adsorption appears in most samples, even when their curves reach the saturated vapor pressure ($P/P_0=1.0$), which indicates the presence of mesopores and macropores in the samples. The desorption isotherms of the shale samples in the study area differ from the adsorption isotherms starting at a relative pressure of approximately 0.4, forming a distinct hysteresis loop. The shape and area of the hysteresis loop effectively reflects the pore structure characteristics of the sample. The IUPAC classifies four types of hysteresis loops; however, due to the diversity of pore types within rock samples, the actual measured hysteresis loop is often a superposition of multiple standard loops. The shale samples in the study area can be divided into two categories based on the shape of their hysteresis loops.

The hysteresis loop of the first type of shale is the H3 type in the IUPAC classification (Fig. 8b). Overall, the desorption curve is similar to the adsorption curve, forming a narrow hysteresis loop. There is a hysteresis loop in the high-pressure zone, and the adsorption and desorption branches have a large slope, indicating that there were open macropores, such as trough-like pores. As the relative pressure decreases, the slopes of the curves tend to become less steep and the slopes nearly coincide in the low-temperature zone, indicating that the small pore size range is dominated by air-tight pores closed on one end. The pores are primarily wedge-shaped pores open at both ends and groove-like pores composed of flakey particles, which correspond to the interlayer pores of the clay minerals, the slit-shaped pores in the organic matter, and the micro fractures in the matrix.

The hysteresis loop of the second type of shale (10.3%) is similar to the H2 type in the IUPAC classification, but it also has characteristics of the H3 type (Fig. 8c). The desorption branch of this type of curve initially decreases slowly, exhibiting a gentle slope at higher pressures. Then it starts to descend at an accelerated speed at a relative pressure of 0.8. Finally, it coincides with the adsorption curve at a relative pressure of approximately 0.5. The area of the hysteresis loop of this type of shale is significantly larger than that of the first type of shale, indicating that the pores have a complex structure. The pore structure is dominated by narrow-necked, wide-bodied, ink bottle-shaped pores, which correspond to interP pores, intercrystalline pores, and OM pores. Some wedge-shaped pores and groove-like pores composed of flakey particles are also present.

3.4.2 Specific surface area and pore volume

The results of the CO_2 and N_2 adsorption experiments are shown in Table 3 (Zhang et al., 2016b; Ji et al., 2016; Wang et al., 2018; Feng et al., 2018). The average pore volume of the shale in the Bohai Bay Basin is 0.0062 to 0.0127 cm^3/g (Table 3). On average, the micropore, mesopore, and macropore volume account for 15.41%, 60.08%, and 23.36% of the total pore volume, respectively. Overall, the mesopores contribute the most to the total pore volume of the shale in the Bohai Bay Basin, with the mesopore volume of some samples accounting for more than 80% of the total pore volume. In contrast, the contributions of the micropores and macropores are relatively small.

On average, the specific surface area of the shale in the Bohai Bay Basin is 3.618 to 8.565 m^2/g. On average,

the specific surface areas of the micropores, mesopores, and macropores account for 52.29%, 44.59%, and 3.11% of the total specific surface area, respectively. Thus, the micropores and mesopores provide most of the specific surface area of the shale in the Bohai Bay Basin, while the macropores contribute less than 5% of the total specific surface area.

Table 3 Pore structure parameters of the shale in the Bohai Bay Basin

Category	Basin/Depression	Layer	Pore volume (cm^3/g)	Pore volume percent(%)			Surface area (m^2/g)	Surface area percent(%)			Average pore size (nm)
				Micro-pore	Meso-pore	Macro-pore		Micro-pore	Meso-pore	Macro-pore	
Bohai Bay Basin lacustrine shale	Cangdong Depression	Ek_2	0.0088	18.39	48.28	29.80	6.335	66.01	32.51	1.48	3.94
	Dongying Depression	$Es_3+Es_4^U$	0.0127	24.29	51.15	24.56	8.565	78.33	18.74	2.93	3.99
	Zhanhua Depression	$Es_3+Es_4^U$	0.0062	3.53	80.81	15.72	3.618	12.54	82.53	4.93	
Others	Southern Sichuan Basin	Qiongzhusi	0.0057	33.16	49.82	17.02	8.568	77.46	22.46	0.08	3.98
	Southeastern Sichuan Basin	Longmaxi	0.0058	32.30			8.196	50.30			
	Ordos Basin	Yanchang	0.0118	10.12	76.69	13.19	8.080	30.27	67.84	1.89	

In summary, the mesopores and micropores are the main contributors to the pore volume and specific surface area of the shale in the Bohai Bay Basin, respectively. Although the macropores provide some of the pore volume, they do not contribute significantly to the specific surface area.

3.4.3 Characteristics of the pore size distribution

Based on the results of the CO_2 and N_2 adsorption experiments, the characteristics of the pore size distribution of the shale in the Bohai Bay Basin were analyzed and compared with those of typical marine shales in North America and southern China. The shale in the Bohai Bay Basin has a complex pore size distribution with multiple peaks in the curve (Fig. 9), and the pore size distribution characteristics of the samples are quite different. The micropores are characterized by multiple peaks and are dominated by three distinct peaks at 0.48–0.51 nm, 0.58–0.62 nm, and 0.79–0.84 nm. The mesopores are characterized by a single distinct peak at 3.7–4.2 nm. There are no fixed peaks in the macropores. In comparison, the size of the micropores in the marine shale in North America is characterized by a single peak at 0.7–1.0 nm, and no distinct mesopore or micropore peaks were present (Wang et al., 2016).

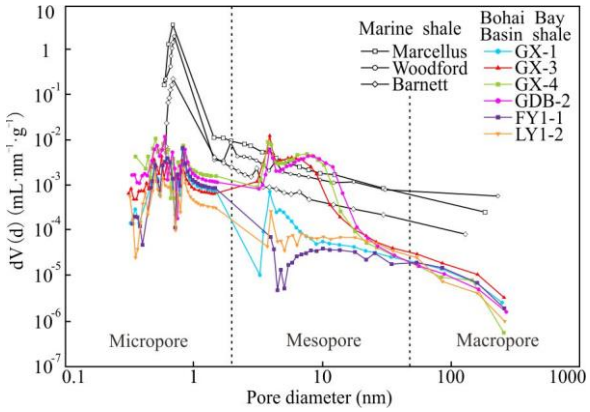

Fig. 9. Pore size distribution characteristics of the shale in the Bohai Bay Basin.

The calculations reveal that the average pore diameter of the shale in the Bohai Bay Basin is 3.94 nm, which is close to those of the shale in the Qiongzhusi Formation in southern Sichuan (3.98 nm), the Longtan Formation (4.66 nm) in southern China, and the Marcellus (3.9 nm) and Barnett (4.0 nm) shales in North America (Chalmers et al., 2012).

4 Discussion

4.1 Main factors controlling reservoir space development

Compared with conventional sandstone reservoirs, the shale oil reservoirs in the Bohai Bay Basin have a wide pore-throat size distribution, diverse pore types, and complex pore structures. Furthermore, the mineral matrix pores and OM pores were co-developed. Overall, the development and evolution of shale oil reservoirs are controlled by multiple factors, including the sedimentary environment, diagenesis, and thermal evolution of the

organic matter during hydrocarbon generation.

4.1.1 Sedimentary environment

Compared with marine shales, continental shales are sensitive to their sedimentary environment. Changes in environmental factors such as climate, salinity, and water column stratification determine, directly or indirectly, the material composition and structure of the rock, thereby controlling the type and location of the microscopic pores (Zhang et al., 2016c). In a humid climate with abundant rainfall, the detrital minerals from the provenance enter the lake basin in large quantities, forming a shale that is rich in brittle minerals such as feldspar and quartz. These rigid frameworks composed of terrestrial brittle minerals are not easily broken during compaction and can therefore support and retain the primary interP pores of the shale.

In a semi-humid climate with stable stratification of lake water, seasonal changes in the sedimentary environment cause rhythmic sedimentation, which successively forms carbonates, detrital minerals, and clay-organic laminae. The laminated organic matter is enriched by high productivity and favorable preservation conditions, leading to the development of OM pores and marginal fractures, which ultimately connect the carbonate dissolution pores and the interP brittle mineral pores in the adjacent laminae, forming a 3D network of connected pores.

In an arid climate, the insufficient input of terrigenous detrital material leads to severe lake salinization. The shale components are dominated by carbonate minerals, and unstable minerals such as calcite and dolomite are easily dissolved by acidic diagenetic fluids during diagenetic evolution. This leads to the formation of dissolution pores on the surfaces and edges of minerals, and results in recrystallization and the formation of intercrystalline pores.

For shales, the salinity of the water during sedimentation directly influences the composition of the diagenetic fluid, which directly controls diagenesis (Luan et al., 2016; Yu et al., 2016). In general, high-salinity brackish water corresponds to an alkaline diagenetic fluid environment, while low-salinity fresh water corresponds to an acidic diagenetic fluid environment. Taking the upper 4^{th} member of the Shahejie Formation in the Dongying Depression as an example, the salinity of the lake during sedimentation was relatively high. The presence of a K^+-rich alkaline diagenetic fluid inhibited the dissolution of feldspar, resulting in a high feldspar content of the shale and a lack of dissolution pores. Conversely, alkaline fluids promote the transformation of clay minerals, especially of montmorillonite to illite, which is accompanied by the formation of many intraP clay mineral pores. In addition, when the Mg^{2+}/Ca^{2+} value of the calcite in the alkaline fluid environment is relatively high, varying degrees of the recrystallization of calcite occurs and a small number of micro fractures and dissolution pores develop.

4.1.2 Diagenesis

(1) Transformation of clay minerals

The clay minerals in the continental shale of the Bohai Bay Basin are mainly composed of illite, montmorillonite, illite/smectite mixed layer, and a small amount of chlorite. The illitization of montmorillonite is the most common and important clay mineral transformation process. In this process, first, the montmorillonite forms the mixed illite/smectite minerals. Then, as the temperature and pressure increase, the structure gradually becomes more orderly. Finally, it is transformed into illite. During this process, the morphology of the minerals transition from flakey to silky as well as thread-like to cotton-like. The illitization of montmorillonite plays a key role in the formation and development of shale pore spaces, not only through the formation of clay pores and shrinkage fractures during the transformation process itself, but also during the migration of chemical components facilitated by the outflow of a large amount of interlayer water that accompanies this process (Wu et al., 2012; Zhang et al., 2016c). Organic matter-rich shale contains abundant organic matter and clay in the form of aggregates. During thermal evolution and hydrocarbon generation, the transformation of montmorillonite to illite can also catalyze hydrocarbon generation from organic matter. The transition of the mixed illite/smectite minerals has a very strong catalytic effect. For example, in wells Fanye-1 and Liye-1 in the Dongying Depression, the high illite content corresponds to the low mixed illite/smectite content and the high porosity, indicating the simultaneous transformation of montmorillonite to illite and hydrocarbon generation from organic matter.

(2) Recrystallization

As mentioned above, the shale of the Bohai Bay Basin contains some carbonate minerals. Most of the calcite and dolomite has a biochemical origin or is formed by late-stage recrystallization. Large amounts of recrystallization can form a specific type of lithofacies; this is evident in the interbedded limestone facies in the Dongying Depression and the block dolomite facies in the Cangdong Depression. Taking the Dongying Depression as an example, the micrite, and microcrystalline, fine-grained, and coarse-grained calcite are developed by different degrees of recrystallization. Morphologically, the recrystallized calcite is primarily composed of granular crystals and a minor amount of columnar fibrous vertical bedding. The recrystallized dolomite in the Cangdong Depression is composed of granular crystals, which are locally enriched in the bedding. In general, the higher the degree of recrystallization, the more developed the intercrystalline pores. Jiang (2014) determined that the degree of recrystallization and the crystal morphology of the calcite are closely related to the organic matter content. When TOC is < 2%, calcite does not recrystallize and is primarily present

as micrite. For 2% < TOC < 4%, the calcite starts to recrystallize and is primarily present as microcrystalline and granular sparite. When TOC is > 4%, significant recrystallization occurs and calcite is primarily present as needle-like columnar crystals.

(3) Dissolution

Dissolution pores are common in shale and usually develop in the interior or on the edges of unstable minerals such as calcite, dolomite, and feldspar. These soluble minerals provide the material basis for the formation of dissolution pores, and the acidic solution produced during diagenesis triggers dissolution. Studies have shown that large amounts of acidic substances, such as organic acids and CO_2, are generated during the thermal evolution of organic matter during hydrocarbon generation (Zhang et al., 2018b). During this process, the ability of the organic acids to provide hydrogen ions is far greater than that of carbonic acid, which is the primary reason dissolution pores develop. In this study, the thermal diagenesis simulation experiment demonstrated that the thermal evolution of organic matter during hydrocarbon generation corresponds to the degree of dissolution. Specifically, when the organic matter reaches maturity and begins to produce organic acid, the dissolution of the carbonate minerals in the shale also occurs. As the temperature and pressure increase, the dissolution rate also increases. Additionally, clay minerals produce acidic fluids during their transformation, which increases the mineral dissolution.

It should be noted that, although the dissolution of shale is very common, some scholars believe that these widely developed dissolved pores do not significantly contribute to the accumulation or migration of hydrocarbons (Zhang, 2018). This is primarily because shale has poor porosity and permeability, and thus, the hydrogen ions in the acidic fluid cannot be replenished fast enough to continue the reaction. In addition, illite forms in the original pores, resulting in dissolution pores that are isolated and have a small-volume. Based on the thermal simulation experiment results, the dissolution pores in the calcite began to gradually merge and connect with each other; however, this only occurred at pressures and temperatures of at least 137.5 MPa and 450°C, respectively.

4.1.3 Thermal evolution during hydrocarbon generation

Thermal evolution of organic matter during hydrocarbon generation is an important factor affecting the formation and evolution of shale reservoirs. It is also the key factor causing the significant difference between the diagenetic evolution paths of shale and conventional sandstone reservoirs. As was previously mentioned, the main diagenetic effects, such as clay mineral transformation, carbonate recrystallization, and unstable mineral dissolution, are inseparable from the effects of thermal evolution during hydrocarbon generation. The source-reservoir integration characteristic of shale also dictates that inorganic diagenesis and organic thermal evolution during hydrocarbon generation are not independent of each other. Instead, they are closely related and interact with each other to jointly control the formation and evolution of the microscopic pores in shale reservoirs (Mastalerz et al., 2013; Li et al., 2015).

Control of shale oil reservoirs by thermal evolution of organic matter during hydrocarbon generation is mainly reflected by three aspects: (1) In the thermal evolution process of organic matter during hydrocarbon generation, the gaseous or liquid hydrocarbons generated by the transformation of solid kerogen are discharged to form internal and organic matter marginal pores. The consumption of water during the hydrocarbon generation process also reduces the volume of the organic matter, and thus, it produces marginal contraction fractures. According to the statistical results, the maturity of the shale in the Bohai Bay Basin is not high. For example, in the low-mature to mature stages of thermal evolution and hydrocarbon generation, the number and size of the internal OM pores differ significantly from those of high maturity marine shales, resulting in a reservoir space dominated by shrinkage fractures on the edges of the organic matter. (2) Thermal evolution of the organic matter during hydrocarbon generation discharges a large amount of organic acids, which makes the diagenetic fluid acidic and provides hydrogen ions and complex metallic elements for the dissolution of unstable minerals such as calcite, dolomite, and feldspar. (3) In addition to the positive effects of the thermal evolution of organic matter on the development of shale pores, after hydrocarbon generation and expulsion from the organic matter in the late stage of diagenesis, the hydrocarbon enriched pores inhibit other diagenesis effects, which is not conducive to the subsequent reformation of pores.

4.2 Diagenetic sequence and reservoir space evolution

Compared with sandstone reservoirs, shale reservoirs follow a different diagenetic evolution pathway due to their closed system and complex composition. The diagenesis of shale in a closed system is almost unaffected by foreign matter, and the various diagenetic effects are interrelated and mutually promoted or inhibited. The product of one diagenetic stage is the reactant of another diagenetic stage, and organic–inorganic synergistic diagenesis results in the formation and evolution of the shale reservoir space being much more complex than that of sandstone reservoirs (Peltonen et al., 2009; Taylor and Macquaker, 2014; Zhai et al., 2018b).

Based on the main factors controlling the development of shale reservoir space, the division marks and schemes for the diagenetic stages of clastic rocks, carbonate rocks, and clay rocks, as well as the petrologic characteristics of the shale oil reservoirs in the Bohai Bay Basin and the diagenetic stages of the shale in the study area are divided based on their burial depth, vitrinite reflectance (R_o), maximum peak temperature (T_{max}), clay mineral composition, and contents of other authigenic minerals. The results show that the main body of

shale in the Bohai Bay Basin is in the middle diagenesis stage, while a small amount of shale is in the late diagenetic stage. Considering factors such as diagenetic stage, diagenetic environment, and stratigraphic burial history, the diagenetic evolution and its influence on reservoir space development are analyzed and the diagenetic sequence and reservoir space evolution path in the Bohai Bay Basin are established (Fig. 10).

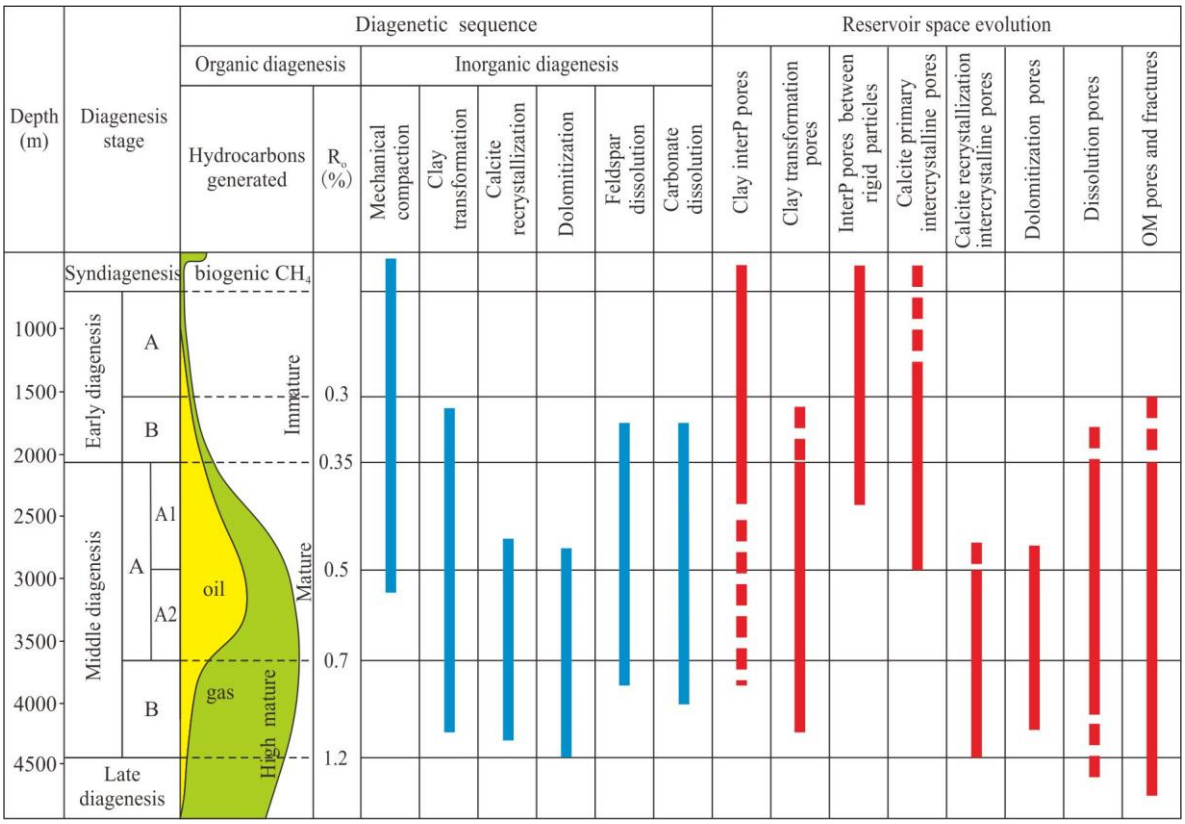

Fig. 10. Diagenetic sequence and reservoir space evolution of the shale in the Bohai Bay Basin.

During stage A of early diagenesis, after sedimentation and consolidation, the diagenesis is dominated by mechanical compaction. As the overburden pressure increases, the number and volume of pores dominated by the interP pores of felsic minerals decreases rapidly as the interP water is discharged.

During stage B of early diagenesis, mechanical compaction is the main type of diagenesis, and the porosity continues to decrease. Montmorillonite begins to transform into illite, locally producing intraP pores and shrinkage fractures, and the interlayer water is discharged. The organic matter is not mature, and only a small amount of organic matter produces organic acids from biological-thermal catalysis, leading to the local dissolution of carbonate minerals and feldspar. In this stage, the reservoir space is mainly composed of interP pores, intraP pores, and intercrystalline calcite pores.

During stage A1 of middle diagenesis, the intercrystalline calcite pores and the interP pores of the felsic minerals gradually shrink, the transformation of the clay minerals continues, and a significant number of intraP pores develop in the clay minerals. At the same time, the intraP pores of some flocculated clay minerals begin to disappear. An important process during this stage is that the organic matter begins to thermally evolve and generate hydrocarbons, forming pores and micro fractures inside and on the edges of the organic matter. This process simultaneously discharges large amounts of organic acids, which dissolve unstable minerals such as feldspar and calcite. The calcite also begins to recrystallize, forming a small number of intercrystalline pores. During this stage, interP pores, intraP pores, dissolution pores, and OM pores also develop within the shale, while the presence of micro fractures provides another channel for the migration of diagenetic fluids.

During stage A2 of middle diagenesis, the transformation of the clay minerals is nearly complete, and illite accounts for over 90% of the clay minerals. As the thermal evolution of organic matter and hydrocarbon generation decreases from the peak values, the dehydration of the clay minerals and the hydrocarbon generation from the organic matter lead to an increase in the shale fluid pressure, which accelerates the formation of micro fractures. The migration and retention of acidic fluids within a pore network composed of micro fractures and pores leads to the dissolution of unstable minerals and the recrystallization of carbonate minerals on a large scale, which changes the original reservoir space. This is the stage in the diagenetic evolution sequence in thich the most significant reformation of the reservoir space occurred.

During stage B of middle diagenesis, the organic matter enters the high maturity stage and the organic matter transitions from primarily generating oil to primarily generating gas. This process forms a number of nanoscale OM pores and significantly decreases the median radius of the shale pores. During this process, a decrease in the

discharge of organic acids leads to a decrease in the amount of dissolution pores. In addition, the diagenetic fluid changes from an acidic environment to a weakly alkaline environment and the fluids tend to be saturated, causing the cementation and precipitation of authigenic minerals, which fill the original pores and fractures. During this stage, as a result of multiple effects, the number of types of shale reservoir spaces decreases, the volume becomes smaller, and the overall porosity decreases.

5 Conclusions

(1) The microscopic pores in shale can be divided into three broad categories: mineral matrix pores, OM pores, and micro fractures. Based on the location and genetic mechanism of the pores, they can be further subdivided into seven categories and fourteen sub-categories. Mineral matrix pores include interP pores, intraP pores, intercrystalline pores, and dissolution pores. The OM pores are mainly secondary OM pores produced during the thermal evolution of organic matter, whereas the micro fractures can be divided into fractures created by tectonic genesis and those created by diagenesis. There are differences in the distribution and connectivity of the reservoir spaces of the different samples analyzed in this study.

(2) The shale reservoir in the Bohai Bay Basin has a complex pore structure, which can be divided into two categories based on the shape of the adsorption loop. The pores are mainly wedge-shaped, flat slit-shaped, and ink bottle-shaped. The total pore volume and total specific surface area are between 0.0062 and 0.0127 cm^3/g, and 3.618 and 8.565 m^2/g, respectively. The average pore diameter is approximately 3.94 nm. Mesopores and micropores are the main contributors to pore volume and specific surface area, respectively Macropores provide some of the pore volume, but do not significantly contribute to the specific surface area.

(3) The development and evolution of shale oil reservoirs are controlled by multiple factors such as the sedimentary environment, diagenesis, and thermal evolution during hydrocarbon generation. Among these factors, the sedimentary environment determines the composition and structure of the shale and provides the material basis for shale pore development. Diagenesis controls the type and characteristics of the pores, and the thermal evolution of the organic matter is closely related to inorganic diagenesis, which synergistically drives the formation and evolution of the pores. Stages A and B of middle diagenesis are the key periods in which the evolution of the shale reservoir space occurred.

Acknowledgements

This study was supported by the National Natural Science Foundation of China (Grant No. 41572087). We would like to thank the reviewers for their constructive comments, which significantly improved the manuscript.

References

Aplin, A.C., and Macquaker, J.S.H., 2011. Mudstone diversity: Origin and implications for source, seal, and reservoir properties in petroleum systems. *AAPG Bulletin*, 95(12): 2031–2059.

Bai, B., Zhu, R.K., Wu, S.T., Yang, W.J., Gelb, J., Gu, A., Zhang, X.X., and Su, L., 2013. Multi-scale method of Nano(Micro)-CT study on microscopic pore structure of tight sandstone of Yanchang Formation, Ordos Basin. *Petroleum Exploration and Development*, 40(3), 329–333 (in Chinese with English abstract).

Bao, S.J., Zhai, G.Y., Zhou, Z., Yu, S.F., Chen, K., Wang, Y.F., Wang, H., and Liu, Y.M., 2018. The evolution of the Huangling uplift and its control on the accumulation and preservation of shale gas. *China Geology*, 1(3), 346–353.

Brooks, B. T., 1952. Evidence of catalytic action in petroleum formation. *Industrial & Engineering Chemistry*, 44(11): 2570–2577.

Brunauer, S., Emmett, P.H., and Teller. E., 1938. Adsorption of gases in multimolecular layers. *Journal of the American chemical society*, 60(2): 309–319.

Chalmers, G.R., and Bustin, R.M., 2012. Light volatile liquid and gas shale reservoir potential of the Cretaceous Shaftesbury Formation in northeastern British Columbia, Canada. *AAPG bulletin*, 96(7): 1333–1367.

Chalmers, G.R., Bustin, R.M., and Power, I.M., 2012. Characterization of gas shale pore systems by porosimetry, pycnometry, surface area, and field emission scanning electron microscopy/transmission electron microscopy image analyses: Examples from the Barnett, Woodford, Haynesville, Marcellus, and Doig units. *AAPG bulletin*, 96(6): 1099–1119.

Chen, L., Jiang, Z.X., Liu, K.Y., Gao, F.L., and Wang, P.F., 2017. A combination of N_2 and CO_2 adsorption to characterize nanopore structure of organic‐rich Lower Silurian Shale in the Upper Yangtze Platform, South China: implications for shale gas sorption capacity. *Acta Geologica Sinica* (English Edition), 91(4): 1380–1394.

Chen, F.W., Lu, S.F., and Ding, X., 2018. Pore types and quantitative evaluation of pore volumes in the Longmaxi Formation shale of southeast Chongqing, China. *Acta Geologica Sinica* (English Edition), 92(1): 342–353.

Chen, X.H., Luo, S.Y., Liu, A., and Li, H., 2018a. The oldest shale gas reservoirs in southern margin of Huangling uplift, Yichang, Hubei, China. *China Geology*, 1(1), 158–159.

Chen, X.H., Wei, K., Zhang, B.M., Li, P.J., Li, H., Liu, A., and Luo, S.Y., 2018b. Main geological factors controlling shale gas reservoir in the Cambrian Shuijingtuo Formation in Yichang of Hubei Province as well as its and enrichment patterns. *Geology in China*, 45(2): 207–226(in Chinese with English abstract).

Curtis, M.E., Cardott, B.J., Sondergeld, C.H., and Rai, C.S., 2012a. Development of organic porosity in the Woodford Shale with increasing thermal maturity. *International Journal of Coal Geology*, 103(2): 26–31.

Curtis, M.E., Sondergeld, C.H., Ambrose, R.J., and Rai, C.S., 2012b. Microstructural investigation of gas shales in two and three dimensions using nanometer–scale resolution imaging. *AAPG Bulletin*, 96(4): 665–677.

Desbois, G., Urai, J.L., and Kukla, P.A., 2009. Morphology of the pore space in claystones–evidence from BIB/FIB ion beam sectioning and cryo–SEM observations. *Earth*, 4(1): 15–22.

Feng, X.L., Ao, W.H., and Tang, X., 2018. Characteristics of pore development and its main controlling factors of

continental shale gas reservoirs : A case study of Chang 7 Member in Ordos Basin. *Journal of Jilin University* (Earth Science Edition), 48(3): 678–692.
Fishman, N.S., Hackley, P.C., Lowers, H.A., Hill, R.J., Egenhoff, S.O., Eberl, D.D., and Blum, A.E., 2012. The nature of porosity in organic–rich mudstones of the Upper Jurassic Kimmeridge Clay Formation, North Sea, offshore United Kingdom. *International Journal of Coal Geology*, 103(2): 32–50.
Gale, J.F., Reed, R.M., and Holder, J., 2007. Natural fractures in the Barnett Shale and their importance for hydraulic fracture treatments. *AAPG Bulletin*, 91(4): 603–622.
Gregg, S.J., and Sing, K.S.W., 1982. *Adsorption, Surface Area and Porosity* (2nd ed). New York: Academic Press, 107.
Gu, X., Cole, D.R., Rother, G., Mildner, D.F., and Brantley, S.L., 2015. Pores in Marcellus shale: a neutron scattering and FIB–SEM study. *Energy & Fuels*, 29(3): 1295–1308.
Hillier, S., 2002. Quantitative analysis of clay and other minerals in sandstones by X‐ray powder diffraction (XRPD). *Clay Mineral Cements in Sandstones: Special Publication*, 34: 213–251.
Hu, S.Y., Zhu, R.K., Wu, S.T., Bai, B., Yang, Z., and Cui, J.W., 2018. The exploration and development of continental tight oil in China under the background of low oil price. *Petroleum Exploration and Development*, 45(4): 1–12 (in Chinese with English abstract).
Huang, X., Zhang, J.C., Li, X.G., Sun, R., Peng, J.L., and Long, S., 2015. Pore types and characteristics of continental shale and discussion on the process of oil and gas accumulation: A case study of the Western Sag of Liaohe Depression. *Natural Gas Geoscience*, 26(7): 1422–1432 (in Chinese with English abstract).
Javadpour, F., Moravvej Farshi, M., and Amrein, M., 2012. Atomic–force microscopy: a new tool for gas–shale characterization. *Journal of Canadian Petroleum Technology*, 51(04): 236–243.
Ji, W.M., Song, Y., Jiang, Z.X., Chen, L., Wang, P.F., Liu, Q.X., Gao, F.L., and Yang, X., 2016. Micro-nano pore structure characteristics and its control factors of shale in Longmaxi Formation, southeastern Sichuan Bain. *Acta Petrolei Sinica*, 37(2): 182–195 (in Chinese with English abstract).
Jia, C.Z., 2017. Breakthrough and significance of unconventional oil and gas to classical petroleum geological theory. *Petroleum Exploration and Development*, 44(1): 1–11 (in Chinese with English abstract).
Jiang, Z.X., Zhang, W.Z., Liang, C., Wang, Y.S., Liu, H.M., and Chen, X., 2014. Characteristics and evaluation elements of shale oil reservoir. *Acta Petrolei Sinica*, 35(1): 184–196 (in Chinese with English abstract).
Johns, W.D., 1979. Clay mineral catalysis and petroleum generation. *Annual Review of Earth and Planetary Sciences*, 7(1), 183–198.
Li, A., Ding, W., He, J., Dai, P., Yin, S., and Xie, F., 2016. Investigation of pore structure and fractal characteristics of organic – rich shale reservoirs: A case study of lower Cambrian Qionzhusi formation in Malong block of eastern Yunnan Province, South China. *Marine and Petroleum Geology*, 70: 46–57.
Li, C., Zhu, X.M., Zhu, S.F., Geng, M.Y., Bi, Y.Q., Shu, Q.L., and Xu, F.G., 2015. Shale Reservoir Characteristics of the Lower 3th Member of Shahejie Formation, Luojia Area, Zhanhua Sag. *Acta Sedimentologica Sinica*, 33(4): 795–808 (in Chinese with English abstract).
Liang, C., Jiang, Z., Cao, Y., Wu, M., Guo, L., and Zhang, C., 2016. Deep–water depositional mechanisms and significance for unconventional hydrocarbon exploration: A case study from the lower Silurian Longmaxi shale in the southeastern Sichuan Basin. *AAPG Bulletin*, 100(5): 773–794.
Lin, W., 2016. A review on shale reservoirs as an unconventional play–the history, technology revolution, importance to oil and gas industry, and the development future. *Acta Geologica Sinica* (English Edition), 90(5): 1887–1902.
Liu, B., Shi, J.X., Fu, X.F., Lyu, Y.F., Sun, X.D., Gong, L., and Bai, Y.F., 2018. Petrological characteristics and shale oil enrichment of lacustrine fine-grained sedimentary system: A case study of organic-rich shale in first member of Cretaceous Qingshankou Formation in Gulong Sag, Songliao Basin, NE China. *Petroleum Exploration and Development*, 45(05):828–838 (in Chinese with English abstract).
Liu, B., Lyu, Y.F., Meng, Y.L., Li, X.N., Guo, X.B., Ma, Q., and Zhao, W.C., 2015. Petrologic characteristics and genetic model of lacustrine lamellar fine-grained rock and its significance for shale oil exploration: A case study of Permian Lucaogou Formation in Malang sag, Santanghu Basin, NW China. *Petroleum Exploration and Development*, 42(5): 598–607 (in Chinese with English abstract).
Loucks, R.G., Reed, R.M., Ruppel, S.C., and Jarvie, D.M., 2009. Morphology, genesis, and distribution of nanometer–scale pore in siliceous mudstones of the Mississippian Barnett shale. *Journal of Sedimentary Research*, 79(12): 848–861.
Loucks, R.G., Reed, R.M., Ruppel, S.C., and Hammes, U., 2012. Spectrum of pore types and networks in mudrocks and a descriptive classification for matrix–related mudrock pores. *AAPG Bulletin*, 96(6): 1071–1098.
Luan, G.Q., Dong, C.M., Ma, C.F., Lin, C.Y., Zhang, J.Y., Lyu, X.F., and Muhammad, A.Z., 2016. Pyrolysis Simulation Experiment Study on Diagenesis and Evolution of Organic-rich Shale. *Acta Sedimentologica Sinica*, 34(6):1208–1216 (in Chinese with English abstract).
Ma, C., Elsworth, D., Dong, C., Lin, C., Luan, G., Chen, B., Liu, X., Muhammad, J.M., Muhammad, A.Z., Shen, Z., and Tian, F., 2017. Controls of hydrocarbon generation on the development of expulsion fractures in organic–rich shale: Based on the Paleogene Shahejie Formation in the Jiyang Depression, Bohai Bay Basin, East China. *Marine and Petroleum Geology*, 86: 1406–1416.
Macquaker, J.H., and Adams, A.E., 2003. Maximizing information from fine–grained sedimentary rocks: An inclusive nomenclature for mudstones. *Journal of Sedimentary Research*, 73(5): 735–744.
Mastalerz, M., He, L., Melnichenko, Y.B., and Rupp, J.A., 2012. Porosity of coal and shale: Insights from gas adsorption and SANS/USANS techniques. *Energy & Fuels*, 26(8): 5109–5120.
Mastalerz, M., Schimmelmann, A., Drobniak, A., and Chen, Y., 2013. Porosity of Devonian and Mississippian New Albany Shale across a maturation gradient: Insights from organic petrology, gas adsorption, and mercury intrusion. *AAPG Bulletin*, 97(10): 1621–1643.
Milliken, K.L., Rudnicki, M., Awwiller, D.N., and Zhang, T., 2013. Organic matter–hosted pore system, Marcellus Formation (Devonian), Pennsylvania. *AAPG Bulletin*, 97(2): 177–200.
Milner, M., McLin, R., and Petriello, J., 2010. Imaging texture and porosity in mudstones and shales: Comparison of secondary and ion-milled backscatter SEM methods. In *Canadian unconventional resources and international petroleum conference*. Society of Petroleum Engineers.
Nelson, P.H., 2009. Pore–throat sizes in sandstones, tight sandstones, and shales. *AAPG Bulletin*, 93(3): 329–340.
Nie, H.K., Zhang, P.X., Bian, R.K., Wu, X.L., and Zhai, C.B., 2016. Oil accumulation characteristics of China continental shale. *Earth Science Frontiers*, 23(2): 55–62 (in Chinese with English abstract).
Peltonen, C., Marcussen, Ø., Bjørlykke, K., and Jahren, J., 2009. Clay mineral diagenesis and quartz cementation in mudstones: The effects of smectite to illite reaction on rock properties. *Marine and Petroleum Geology*, 26(6): 887–898.
Rexer, T.F., Mathia, E.J., Aplin, A.C., and Thomas, K.M., 2014. High–pressure methane adsorption and characterization of

pores in Posidonia shales and isolated kerogens. *Energy & Fuels*, 28(5): 2886–2901.
Rouquerol, J., Avnir, D., Fairbridge, C.W., Everett, D.H., Haynes, J.M., Pernicone, N., Ramsay, J.D.F., Sing, K.S.W., and Unger, K.K., 1994. Recommendations for the characterization of porous solids (Technical Report). *Pure and Applied Chemistry*, 66(8): 1739–1758.
Schmitt, M., Fernandes, C.P., da Cunha Neto, J.A., Wolf, F.G., and dos Santos, V.S., 2013. Characterization of pore systems in seal rocks using nitrogen gas adsorption combined with mercury injection capillary pressure techniques. *Marine and Petroleum Geology*, 39(1): 138–149.
Slatt, R.M., and O'Brien, N.R., 2011. Pore types in the Barnett and Woodford gas shales: Contribution to understanding gas storage and migration pathways in fine–grained rocks. *AAPG Bulletin*, 95(12): 2017–2030.
Song, Y., Zhou, L., Guo, X.G., Chang, Q.S., and Wang, X.T., 2017. Characteristics and occurrence of lacustrine dolomitic tight-oil reservoir in the Middle Permian Lucaogou Formation, Jimusaer sag, southeastern Junggar Basin. *Acta Petrologica Sinica*, 33(4): 1159–1170 (in Chinese with English abstract).
Sun, H.Q., 2017. Exploration practice and cognitions of shale oil in Jiyang depression. *China Petroleum Exploration*, 22(4): 1–14 (in Chinese with English abstract).
Teng, C.Y., Zou, H.Y., and Hao, F., 2014. Control of differential tectonic evolution on petroleum occurrence in Bohai Bay Basin. *Science China: Earth Science*, 57: 1110–1128 (in Chinese with English abstract).
Taylor, K.G., and Macquaker, J.H.S., 2014. Diagenetic alterations in a silt- and clay-rich mudstone succession: an example from the Upper Cretaceous Mancos Shale of Utah, USA. *Clay Minerals*, 49(2): 213–227.
Wang, M., Lu, S.F., Wang, Z.W., Liu, Y., Huang, W.B., Chen, F.W., Xu, X.Y., Li, Z., and Li, J.J., 2016. Reservoir characteristics of lacustrine shale and marine shale: Examples from the Songliao Basin, Bohai Bay Basin and Qiannan Depression. *Acta Geologica Sinica* (English Edition), 90(3): 1024–1038.
Wang, Z., Li, X.Q., Qi, S., Yao, S.P., and Wang, F.Y., 2018. Characteristics of microscopic pore structures and its influencing factors of the Qiongzhusi Formation Shales in the Southern Sichuan Basin. *Geological Journal of China Universities*, 24(2): 273–284 (in Chinese with English abstract).
Wei, H.X., Wang, J.J., Zeng, P.S., and Wang, S.Q., 2018. Micropore structure characteristics of Wufeng-Longmaxi Formation black shale along Qilongcun section in northwest Guizhou. *Geology in China*, 45(2): 274–2285(in Chinese with English abstract).
Wu, L.G., Li, X.S., Guo, X.B., Luo, Q.S., Liu, X.J., Chen, X., and Jiang, Z.X., 2012. Diagenetic evolution and formation mechanism of dissolved pore of shale oil reservoirs of Lucaogou formation in Malang sag. *Journal of China University of Petroleum*, 36(3):38–43 (in Chinese with English abstract).
Wu, S.T., Zhu, R.K., Li, X., Jin, X., Yang, Z., and Mao, Z.G., 2018. Evaluation and application of porous structure characterization technologies in unconventional tight reservoirs. *Earth Science Frontiers*, 25(2): 191–203 (in Chinese with English abstract).
Xi, Z.D., Tian, Z.B., and Tang, S.H., 2016. Characteristics and main controlling factors of shale gas reservoirs in transitional facies on the eastern margin of Ordos Basin. *Geology in China*, 43(6): 2059–2069 (in Chinese with English abstract).
Yan, J.H., Pu, X.G., Zhou, L.H., Chen, S.Y., and Han, W.Z., 2015. Naming method of fine-grained sedimentary rocks on basis of X-ray diffraction data. *China Petroleum Exploration*, 20(1): 48–54 (in Chinese with English abstract).
Yang, H., Liang, X.W., Niu, X.B., Feng, S.B., and You, Y., 2017. Geological conditions for continental tight oil formation and the main controlling factors for the enrichment: A case of Chang 7 Member, Triassic Yanchang Formation, Ordos Basin, NW China. *Petroleum Exploration and Development*, 44(1), 11–19 (in Chinese with English abstract).
Yu, B.S., 2013. Classification and characterization of gas shale pore system. *Earth Science Frontiers*, 20(4):211–220 (in Chinese with English abstract).
Yu, K.H., Cao, Y.C., Qiu, L.W., Sun, P.P., Yang, Y.Q., Qu, C.S., Li, Y.W., Wan, M., and Su, Y.G., 2016. Brine evolution of ancient lake and mechanism of carbonate minerals during the sedimentation of Early Permian Fengcheng Formation in Mahu Depression, Junggar Basin, China. *Natural Gas Geoscience*, 27(7):1248–1263 (in Chinese with English abstract).
Zhai, G.Y., Bao, S.J., Pang, F., Ren, S.M., Chen, K., Wang, Y.F., Zhou, Z., and Wang, S.J., 2017. Peservoir-forming pattern of "four-storey" hydrocarbon accumulation in Anchang syncline of northern Guizhou Province. *Geology in China*, 44(1): 1–12(in Chinese with English abstract).
Zhai, G.Y., Wang, Y.F., Zhou, Z., Yu, S.F., Chen, X.L., and Zhang, Y.X., 2018a. Exploration and research progress of shale gas in China. *China Geology*, 1(2), 257–272.
Zhai, G.Y., Wang, Y.F., Zhou, Z., Liu, G.H., Yang, Y.R., and Li, J., 2018b. "Source-Diagenesis-Accumulation" enrichment and accumulation regularity of marine shale gas in southern China. *China Geology*, 1(3), 319–330.
Zhang, Q., Zhu, X.M., Li, C.X., Qiao, L.J.Y., Liu, C., Mei, X.H., Du, H.Y., and Lu, J.J., 2016b. Classification and quantitative characterization of microscopic pores in organic-rich shale of the Shahejie Formation in the Zhanhua Sag, Bohai Bay Basin. *Oil & Gas Geology*, 37(3):422–432 (in Chinese with English abstract).
Zhang, S.M., Cao, Y.C., Jahren, J., Zhu, R.K., Mao, Z.G., Xi, K.L., Muhammad, K., and Hellevang, H., 2018b. Pore Characteristics of the Fine–Grained Tight Reservoirs in the Yabulai Basin, Northwestern China. *Acta Geologica Sinica* (English edition), 92(3): 1170–1192.
Zhang, S., Liu, H.M., Song, G.Q., Wang, Y.S., Chen, S.Y., and Zhang, S.P., 2016c. Genesis and control factors of shale oil reserving space in Dongying Depression. *Acta Petrolei Sinica*, 37(12):1495–1507 (in Chinese with English abstract).
Zhang, S., Liu, H.M., Wang, M., Fu, A.B., Bao, Y.S., Wang, W.Q., Teng, J.B., and Fang, Z.W., 2018a. Pore evolution of shale oil reservoirs in Dongying Depression. *Acta Petrolei Sinica*, 39(7): 754–766 (in Chinese with English abstract).
Zhang, S., 2018. Diagenesis and mechanism of shale reservoir pore increase and reduction in Dongying Depression. *Journal of China University of Mining & Technology*, 47(3): 562–578 (in Chinese with English abstract).
Zhang, X.S., Wang, H.J., Ma, F., Sun, X.C., Zhang, Y., and Song, Z.H., 2016a. Classification and characteristics of tight oil plays. *Petroleum Science*, 13(1), 18–33.
Zhao, X.Z., Wang, Q., Jin, F.M., Luo, N., Fan, B.D., Li, X., Qin, F.Q., and Zhang, H.W., 2015. Re-exploration program for petroleum-rich sags and its significance in Bohai Bay Basin, East China. *Petroleum Exploration and Development*, 42(6):723–733 (in Chinese with English abstract).
Zhao, X.Z., Zhou, L.H., Pu, X.G., Jin, F.M., Han, W.Z., Xiao, D.Q., Chen, S.Y., Shi, Z.N., Zhang, W., and Yang, F., 2018. Geological characteristics of shale rock system and shale oil exploration breakthrough in a lacustrine basin: A case study from the Paleogene 1st sub-member of Kong 2 Member in Cangdong Depression, Bohai Bay Basin, China. *Petroleum Exploration and Development*, 45(3):361–372 (in Chinese with English abstract).
Zhou, L.H., Pu, X.G., Xiao, D.Q., Li, H.X., Guan, Q.S., Lin, L., and Qu, N., 2018. Geological conditions for shale oil formation and the main controlling factors for the enrichment of the 2nd member of Kongdian Formation in the Cangdong Depression, Bohai Bay Basin. *Natural Gas Geoscience*, 29(09): 1323–1332 (in Chinese with English abstract).
Zhu, R.K., Wu, S.T., Su, L., Cui, J.W., Mao, Z.G., and Zhang, X.X., 2016. Problems and future works of porous texture

characterization of tight reservoirs in China. *Acta Petrolei Sinica*, 37(11):1323–1336 (in Chinese with English abstract).
Zou, C.N., Zhu, R.K., Bai, B., Yang, Z., Wu, S.T., Su, L., Dong, D.Z., and Li, X.J., 2011. First discovery of nano-pore throat in oil and gas reservoir in China and its scientific value. *Acta Petrologica Sinica*, 27(6):1857–1864 (in Chinese with English abstract).
Zou, C.N., Zhai, G.M., Zhang, G.Y., Wang, H.J., Zhang, G.H., Li, J.Z., Wang, Z.M., Wen, Z.X., Ma, F., Liang, Y.B., Yang, Z., Li, X., and Liang, K., 2015. Formation, distribution, potential and prediction of global conventional and unconventional hydrocarbon resources. *Petroleum Exploration and Development*, 42(1): 13–25 (in Chinese with English abstract).

About the first author
DENG Yuan, male, born in 1990 in Heze City, Shandong Province; a Ph. D candidate in School of Geosciences, China University of Petroleum (East China). He is now interested in the study on formation mechanisms and characteristics of shale. Email: dengyuan_upc@163.com; phone: 15153226313.

About the corresponding author
CHEN Shiyue, male, born in 1963 in Shangluo City, Shaanxi Province; doctor; graduated from China University of Mining and Technology; professor of China University of Petroleum (East China). He is now interested in the study on sedimentology and reservoir geology. Email: chenshiyue@vip.sina.com; phone: 18253298538.